

Review Article

Review of Modified Nickel-Cobalt Lithium Aluminate Cathode Materials for Lithium-Ion Batteries

Ding Wang,¹ Weihong Liu,¹ Xuhong Zhang,² Yue Huang,¹ Mingbiao Xu ^{1,2}
and Wei Xiao ³

¹School of Petroleum Engineering, Yangtze University, Wuhan 430100, China

²Jingzhou Jiahua Technology Co. Ltd., Jingzhou 434000, China

³School of Chemistry and Environmental Engineering, Yangtze University, Jingzhou 434000, China

Correspondence should be addressed to Mingbiao Xu; xumingbiao2019@126.com and Wei Xiao; xwylyq2006@126.com

Received 4 November 2019; Accepted 4 December 2019; Published 29 December 2019

Guest Editor: Zhangxing He

Copyright © 2019 Ding Wang et al. This is an open access article distributed under the Creative Commons Attribution License, which permits unrestricted use, distribution, and reproduction in any medium, provided the original work is properly cited.

Ternary nickel-cobalt lithium aluminate $\text{LiNi}_x\text{Co}_y\text{Al}_{1-x-y}\text{O}_2$ (NCA, $x \geq 0.8$) is an essential cathode material with many vital advantages, such as lower cost and higher specific capacity compared with lithium cobaltate and lithium iron phosphate materials. However, the noticeably irreversible capacity and reduced cycle performance of NCA cathode materials have restricted their further development. To solve these problems and further improve the electrochemical performance, numerous research studies on material modification have been conducted, achieving promising results in recent years. In this work, the progress of NCA cathode materials is examined from the aspects of surface coating and bulk doping. Furthermore, future research directions for NCA cathode materials are proposed.

1. Introduction

Lithium-ion batteries (LIBs), an energy storage device that combines high-energy density and flexible operation, have been widely used in mobile and wireless electronic devices, power tools, hybrids, and electric vehicles [1–3]. It is known that the performance of LIBs mainly depends on the cathode materials for the battery capacity, and it involves the electrochemical reactions of intercalation and deintercalation of lithium ions. Moreover, the cathode materials play a vital role in their electrochemical performance and account for more than 30% of the cost of the entire battery system. Therefore, it is very important to research and develop cathode materials with high performance and low cost [4, 5].

Layered structural LiCoO_2 materials with a theoretical specific capacity of 274 mAh g^{-1} are the leading cathode in commercial LIBs, such as the first commercial LIBs prepared by Sony in 1991 [6], which can deliver approximately 137 mAh g^{-1} of discharge specific capacity with up to 100% coulombic efficiency. However, the depletion and high cost

of cobalt resources severely restrict practical applications of LiCoO_2 materials [7]. At present, all companies try to avoid using LiCoO_2 and develop new materials with a high potential. LiNiO_2 has the similar structure to LiCoO_2 , and it possesses a higher theoretical specific capacity (275 mAh g^{-1}) at lower cost [8, 9]. However, it is still impossible to synthesize a stoichiometric ratio of LiNiO_2 by a simple process because Ni^{2+} is difficult to completely oxidize to Ni^{3+} , and its electronic structure, magnetic structure, and local structure are still highly controversial, severely limiting this positive electrode from practical applications. It is feasible that a layered nickel-rich oxide replacing Ni with other heteroatoms, such as Co [10, 11], Fe [12, 13], Mn [14, 15], Ti [16], Zr [17], Mg [18], and Al [19], can deliver a sizeable reversible capacity, and it is one of the most attractive strategies in the field of cathode materials. These substitutions mainly affect the layered crystal structure, the electrochemical stability, and the capacity with the intercalation and deintercalation of lithium ions, especially for the thermal stability in the case of extreme charge-discharge processes.

The incorporation of Co significantly enhances the structural order of the nickel-based positive electrode materials [20], which could achieve a high voltage platform. When the molar ratio of Ni and Co components is 8:2, the as-prepared $\text{LiNi}_{0.8}\text{Co}_{0.2}\text{O}_2$ material may possess the best performance and the degree of cation mixing is less than 2% [21]. However, its performance is greatly affected by high temperature. The capacity and potential of the nickel-rich-layered oxide rapidly deteriorate during long-term cycles, which inevitably affect the stable output of energy. The addition of a small amount of Al stabilizes the material structure and improves the thermal stability of the material. The $\text{LiNi}_x\text{Co}_y\text{Al}_{1-x-y}\text{O}_2$ (NCA) material obtained by doping Co and Al elements exhibits exceptional electrochemical properties [22, 23]. Among the series of materials with different ratios of Ni, Co, and Al elements, $\text{LiNi}_{0.8}\text{Co}_{0.15}\text{Al}_{0.05}\text{O}_2$ is the most widely researched material and has attracted full attention and commercialization due to its low cost, nontoxicity, and high-energy density [24]. Tesla is the first company to employ NCA cathode materials to power cars, and it has achieved remarkable success in the electric vehicle industry [25].

NCA is a promising cathode material due to its excellent structural stability and high capacity. However, the cycle and rate performance of NCA materials still limit its large-scale application. The layered rock salt cathode material affects the electrochemical performance due to structural defects. The common structural defects in nickel-based compounds are excess nickel, Li-Ni interlayer mixing, and oxygen vacancy defects [26–28]. The NCA material also has some shortcomings. On the one hand, the poor thermal stability of Ni^{3+} causes the reduction of Ni^{3+} to Ni^{2+} . With the release of Li^+ , some Ni^{2+} ions could easily occupy the vacancy of Li^+ ions during the charging process because the Ni^{2+} radius (0.69 Å) is similar to the Li^+ radius (0.76 Å) [29], which may cause lithium nickel-mixing effects and generate irreversible phases to result in material capacity loss [30, 31]. On the other hand, Ni^{3+} and Ni^{4+} in the high oxidation state are extremely unstable under high-temperature conditions, and they easily react with the HF released by the electrolyte to cause the material structure to change or even collapse, thus affecting the specific capacity and cycle performance of the NCA material [32, 33]. Given these shortcomings, it is necessary to modify the NCA material, and the main modification methods can be summarized and described as surface coating and bulk phase doping.

2. Surface Coating of NCA

To overcome the aforementioned shortcomings of NCA materials, surface coating is a feasible target to lower the electron transport paths, change the transmission mechanism, and improve the electrode material interface reactions. Generally, the coating material needs to present excellent Li^+ and electronic transmission performance, as well as not react with the electrolyte [34, 35]. The surface-coating mechanism of NCA materials can be described in Figure 1, in which the surface coating acts like a shield that protects the structure of the NCA from rogue side reactions. Therefore,

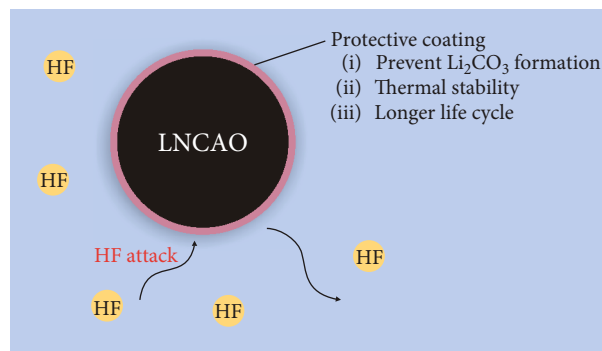


FIGURE 1: Possible function mechanism of NCA material surface coated by carbon.

the cladding layer prevents the crystal structure from collapsing due to corrosion of the positive electrode material and remarkably improves the stability of the battery during the cycle. The surface coating is used to attach the coating material, such as carbon and its derivatives, oxides, phosphates, and active material, to the surface of the cathode material, and it is a straightforward and effective modification method.

2.1. Carbon Coating. Carbon coating is a feasible measure to improve the ionic conductivity and cycle performance of NCA materials under different rates by increasing the electrical conductivity and changing the transmission mechanism [36].

NCA-graphene composite cathode materials are prepared by Yoon et al. [37] using high-energy mechanical milling from the mixture of NCA and graphene at 200 r/min under argon for 30 min. These results can be significantly improved compared with the NCA materials without coating, in which the NCA shows surface resistance of 11.8Ω which is higher than that of the NCA-graphene composite (7.7Ω). The characterization results show that the assembled battery can present excellent physicochemical and battery performance. Between 4.3 and 3 V at a constant current of 55.6 mA/g at 25°C, the NCA delivers a capacity of 172 mAh g^{-1} with a capacity retention of 91%, while the NCA-graphene composite shows a capacity of 180 mAh g^{-1} with a capacity retention of 97% after 80 cycles. The reasons can be mainly attributed to the graphene coating on the surface of NCA materials. On the one hand, the coating graphene can improve the surface conductivity of materials [38, 39]. On the other hand, the graphene layer provides a certain protection to the material and improves the cycle performance. These phenomena can be also detected and elaborated in the references. For example, Chung et al. [40] have adopted sodium dodecyl sulfate as the carbon source, as well as the NCA materials evenly mixed with sodium dodecyl sulfate in the air at 600°C for 5 h to get carbon-coated NCA/C materials. The capacity retention rate of NCA/C is 93% after 40 cycles at 0.1 C, which is higher than that of the uncoated material (86%). Liu et al. [41] reported the coated NCA composite material using 1.0 wt % sucrose and glucose as carbon sources after being calcined at 600°C for 4 h in an argon

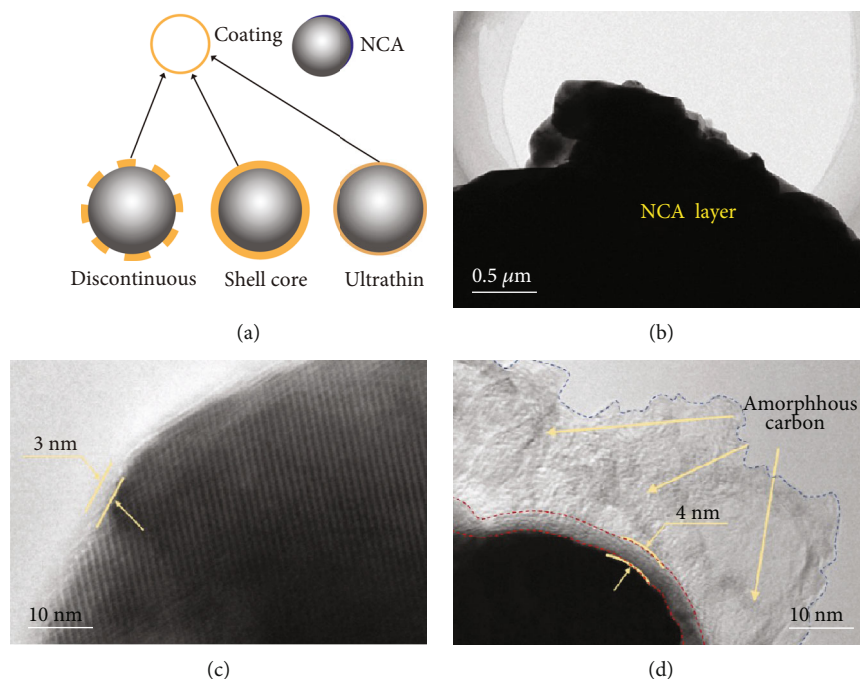


FIGURE 2: Types of electrode material surface coating (a). TEM images of NCA coated with different carbon sources: (b) bare; (c) glucose 1% NCA/C; (d) sucrose 1% NCA/C [41].

atmosphere. The battery performance indicates that the capacity retention of the composite cathodes coated by sucrose and glucose is about 88.3% and 70.4% after 200 cycles at 1.0 C, respectively, which are clearly higher than the uncoated one. Moreover, the battery performance can be tailored by the thickness of the carbon layer, which can be significantly observed by TEM technique. Figure 2 displays the TEM images of NCA materials coated by different carbon sources.

The amorphous carbon coating may cause more unfavorable Ni^{2+} content and exacerbate the $\text{Li}^+/\text{Ni}^{2+}$ intermixing degree, resulting in the degradation of battery performance of NCA cathode material [42, 43]. The reason can be attributed to the reduction of Ni^{3+} to Ni^{2+} by the in situ carbonization of the carbon source. He et al. [44] developed an alternative method for carbon material coating without in situ carbonization and used separately synthesized graphene nanodots (GND) for the non-in situ coating process of NCA cathode materials. The study results show that the uniform distribution of 5 nm GND on the surface of $\text{LiNi}_{0.8}\text{Co}_{0.15}\text{Al}_{0.05}\text{O}_2$ particles can significantly improve the electron conductivity and exhibit a high discharge specific capacity of 150 mAh g^{-1} at 5.0 C. The carbon coating improves the electron transport path on the surface of the NCA, transforms point-to-point conduction into face-to-face conduction, and significantly improves the conductivity, and the cycle performance of the material is also improved under high rate conditions. Moreover, it is worth noting that the carbon layer doped with N and P elements could improve the electrical conductivity of the materials by increasing the local electron density of the carbon material. Gao et al. [45] prepared high performance $\text{LiNi}_{0.8}\text{Co}_{0.15}\text{Al}_{0.05}\text{O}_2$ materials by coating the nitrous and phosphorus codoped nanocarbon

coating (N/PC) on the surface, and the aniline was used as carbon source and nitrogen source and phytic acid as carbon source and phosphorus source. When the N/PC coating amount was up to 1.0 wt %, the materials can deliver the best electrochemical performance in which the capacity retention can retain at 90.7% after 200 cycles at 1.0 C that was significantly over 70.1% of the uncoated one.

2.2. Oxide Coating. As far as we know, oxides, such as Al_2O_3 , MgO , TiO_2 [46], ZnO , ZrO_2 [47], SiO_2 , CeO_2 , and RuO_2 [48], can be widely used to modify the surface of NCA materials due to excellent electronic conductivity and good compatibility with electrolytes, which can significantly improve the cycle performance and rate performance of NCA materials by enhancing the electron transport and structural stability.

Xie et al. [49] proposed to prepare the SnO_2 -coated Li-excess NCA material by synchronous bifunctional modification via the oxalate coprecipitation route. This bifunctionally modified NCA material can not only exhibit improved electrochemical performance but also exhibit improved storage stability. After 400 cycles at 1.0 C, the capacity decreases from 123.7 to 86.7 mAh g^{-1} with a capacity retention of 70.1%, in which excessive Li is believed to reduce the cationic mixing and SnO_2 modification is deemed to restrict the undesirable side reaction between active materials and electrolytes [50]. Liu et al. [51] have synthesized a multifunctional TiO_2 composite layer by the solid-state reaction to modify $\text{LiNi}_{0.8}\text{Co}_{0.15}\text{Al}_{0.05}\text{O}_2$ materials to enhance the surface and structural stability confirmed by electron microscopy and XPS measurements, in which the substitution of Ti in the crystal structure realizes the synergistic effect of the composite layer and titanium doping by enhancing surface and

structural stability via heterogeneous layer coating and bulk doping [52], and the electrochemical battery exhibits the highest initial capacities of 162.9 and 182.4 mAh g⁻¹ at 1.0 C and 0.1 C, and the discharge capacity retentions can reach 85.0% after 200 cycles at 1.0 C. Moreover, metal oxides doped with different metal elements can provide higher electronic conductivity. He et al. [53] adopted electronically conductive antimony-doped tin oxide (ATO) to coat the NCA cathode material by a wet chemical process. After being coated, the as-prepared ATO-coated NCA (ATO-NCA) material had a high discharge specific capacity of 145 mAh g⁻¹ at a rate of 5.0 C, which is higher than that of the original NCA material (135.2 mAh g⁻¹). In addition, at 60°C and 1.0 C, the ATO-NCA material delivered the capacity retention of 91.7% after 200 cycles, which is much higher than that of the original NCA (70.9%). The significant improvements in cyclic and rate performance are mainly attributed to the ATO coating, which not only enhances electron transport but also effectively inhibits the adverse reactions between NCA materials and electrolytes. At the same time, the Li⁺/Ni²⁺ mixing of the NCA material and the growth of the solid electrolyte interface (SEI) film can be effectively suppressed, and the cycle stability is significantly improved, especially at higher temperatures.

The oxide can also be coated directly with the cathode materials for sintering a precursor and colithium. An advantage of this new coating method is that it makes the coating uniform. Another is that the simultaneous production of the cathode material and the formation of the coating at the same heat treatment temperature result in a strong bond between the coating layer and the substrate. Therefore, the modified cathode material possesses a stable structure and exhibits excellent electrochemical performance during repeated charge and discharge. Zheng et al. [54] used the tetraethyl silicate (TEOS) as a silicon source to transform into a SiO₂ layer on the NCA(OH)₂ precursor surface. Then, the SiO₂-coated NCA(OH)₂ was mixed with Li salt and sintered to obtain a NCA composite directly. The rate and cycling performance of NCA are found to be successfully enhanced, especially in the sample with 3 mol % coating. In addition, due to the high-temperature treatment, Al was doped to SiO₂ as a fast ionic conductor. The result was an effective increase in the diffusion of lithium ions between the electrode and the electrolyte interface while protecting the body from direct contact with the electrolyte. Finally, the stability of the material was increased.

2.3. Phosphate Coating. Surface modification by phosphate has received widespread attention in recent years. The principle of phosphate-coated positive electrode material is the same as that of oxide coating, in which the phosphate has better ion transportability and thermal stability that can better improve the rate performance of the material. The commonly used phosphates are AlPO₄ [55], Li₃PO₄ [56, 57], Ni₃(PO₄)₂ [58], Co₃(PO₄)₂ [59], and so on.

Tang et al. [60] first coated an appropriate amount of NH₄H₂PO₄ on the surface of Ni_{0.815}Co_{0.15}Al_{0.035}(OH)₂ and then sintered it with Li₂CO₃ to prepare the composite (P-NCA), in which NH₄H₂PO₄ can react with residual lith-

ium on the surface of the material to form a uniform Li₃PO₄ coating. The removal of lithium ions and the formation of the ion-conductive coating Li₃PO₄ promoted the transport of Li⁺ to some extent. However, due to the limitation of lithium ion conductivity, the heavy Li₃PO₄ coating inevitably hindered the migration of lithium ions. The cycle stability of the coated LiNi_{0.815}Co_{0.15}Al_{0.035}O₂ at room temperature and 55°C can be improved when the coating content reaches 3 wt %, at which point the DSC shows that the heat generation is considerably decreased from 757 J g⁻¹ to 525 J g⁻¹ for NCA and P-NCA. Qi et al. [55] successfully improved the electrochemical performance of LiNi_{0.8}Co_{0.15}Al_{0.05}O₂ coated with AlPO₄ composite by the wet coating process. The capacity retention was 86.9% after 150 cycles at 0.5 C, which is significantly higher than the 66.8% of the uncoated sample. In addition, the modified sample had better thermal stability and smaller resistance and charge transfer resistance, and the values of R₁ (0.569 Ω) and R₂ (51.6 Ω) of the coated sample were clearly smaller than those of the pristine sample (1.30 Ω and 83.7 Ω, respectively). This improved performance can be mainly attributed to the stable protective layer which can inhibit adverse reactions between NCA and electrolytes.

The phosphate coating can also improve the cycling performance of NCA in a wider cut-off voltage range. Liu et al. [61] first extended the charge and discharge cut-off voltage range to 1.5–4.8 V (vs. Li/Li⁺) and prepared BiPO₄-coated NCA by a coprecipitation method, in which the assembled battery can deliver an initial discharge capacity of 325.0 mAh g⁻¹. It is very encouraging that the first two cycle discharge capacities surpassed the theoretical capacity of NCA (274 mAh g⁻¹) when the cut-off voltage was 1.5–4.8 V. These exceptionally high capacities may be caused by the formation of lithium-rich compounds during the charge and discharge process which is under further exploration. The most significant finding is that the charge and discharge platforms can be found at 2.3–2.5 V and 1.7 V, respectively, which contributes to the high capacity properties of NCA. Additionally, the existence of the BiPO₄ coating effectively protects NCA from electrolyte corrosion and improves the cycle performance of NCA. After the first 30 cycles, the capacity retention of BiPO₄-coated NCA materials increases to 81.48, 77.98, 75.20, and 69.11% in the voltage range of 1.5–4.3 V, 1.5–4.5 V, 1.5–4.6 V, and 1.5–4.8 V, respectively, while that of unmodified NCA materials was 77.99%, 72.08%, 63.35%, and 52.05% in the same voltage ranges.

With the expansion of LiFePO₄-positive materials, FePO₄ can potentially be used as a precursor for the preparation of LiFePO₄-positive materials, which has certain electrochemical activities. Therefore, surface modification by FePO₄ can effectively improve the cycling and thermal stability of NCA materials. Generally, there are two topics in terms of FePO₄ materials in LIBs, namely, uniformly distributed and highly crystalline nano-FePO₄ preparation and uniform surface moderation. Xia et al. [62] employed a general liquid-phase technology to prepare uniformly distributed and highly crystalline nano-FePO₄ powders, which were then used to coat the surface of LiNi_{0.8}Co_{0.15}Al_{0.05}O₂ (NCA) to adjust the interface property between electrodes and electrolytes. Among the samples with different coated FePO₄ contents,

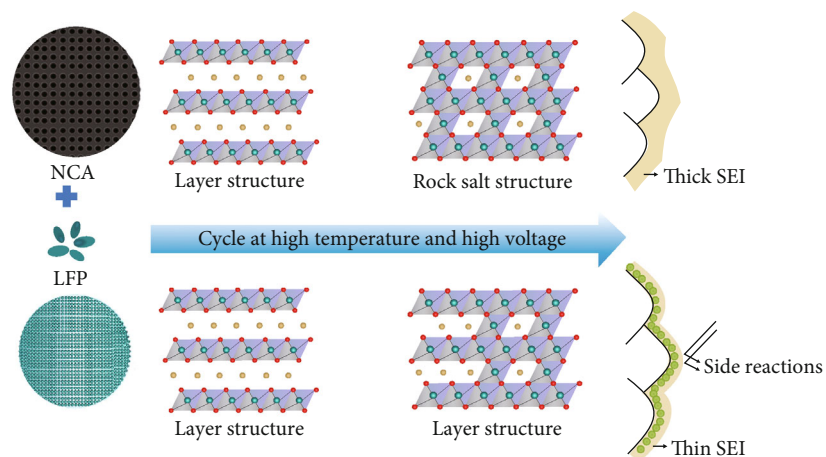


FIGURE 3: A scheme illustrating the effects of a lithium iron phosphate coating on NCA cathodes [68].

the cells with the NCA coated with 2 wt % FePO_4 presented the best electrochemical performance with an initial discharge specific capacity of 181.4 mAh g^{-1} and a capacity retention of 80.49% after 100 cycles at 1.0 C. Moreover, the solid-liquid interface membrane impedance (R_f) changed little during the cycles by the charge transfer resistance fitted from EIS patterns; however, the charge transfer resistance (R_{ct}) of the pristine sample clearly increased from 85Ω to 187Ω while the R_{ct} of the 2 wt % FePO_4 -coated samples increased only slightly. These results reveal that the amorphous FePO_4 coating plays a key role to suppress R_{ct} from increasing during charge-discharge cycles by reducing the charge transfer resistance.

2.4. Active Material Coating. Different from other coatings, active materials, as conductor materials of Li^+ , can better realize the insertion and extraction of Li^+ and improve the cycle performance and rate performance of NCA materials. At the same time, some lithium compounds can be used as electrode materials [63, 64], contributing capacity during charging and discharging cycles, thus reducing the impact of coating on the overall capacity loss of the material. Liu et al. [65] coated 3.0 wt % LiCoO_2 on the surface of NCA material by a molten salt method. Between 2.75 and 4.3 V and at 0.5 C, the initial discharge specific capacity of NCA/ LiCoO_2 material was 163.6 mAh g^{-1} and the capacity retention rate was 95.8% after 50 cycles, whereas the undischarged material had an initial discharge specific capacity of 154.3 mAh g^{-1} and a capacity retention rate of 87.9%. The cycle and rate performance of the coated material were improved. The electrochemical impedance test results showed that the reduction of the NiO phase formed on the surface of the cladding was the main reason for the improved material properties.

NCA is a secondary particle aggregated by primary particles, and its structure has a significant influence on electrochemical performance, such as rate performance and cycle life. During the charge and discharge process, the internal stress of the positive electrode material changes due to the interaction between the lithium ions and the lattice structure, and this stress may cause structural damage of the secondary

particles and accelerate the formation of cracks, yielding the material and the electrolyte. The side reaction is intensified. Yang et al. [66] introduced a filling and coating method using $\text{LiNi}_{0.333}\text{Co}_{0.333}\text{Mn}_{0.333}\text{O}_2$ to fill and coat the surface of the positive electrode material $\text{LiNi}_{0.815}\text{Co}_{0.15}\text{Al}_{0.035}\text{O}_2$; the thickness of the gap layer was approximately 10 nm, there was no capacity loss, and the capacity retention was 88.5% after 200 cycles. The cycle performance was greatly improved, and the polarization was significantly reduced compared with the original NCA. Furthermore, the mechanism of secondary particle fragmentation was further revealed by the in situ compression test. The secondary particle fracture is considered a fatigue process under long-term electrochemical reaction. The coated sample has a good elastic recovery ability, and the NCA with a filled coating can ensure a low residual lithium content and ensure a strong bonding force between adjacent crystal grains, which also improves the long-term cycle stability. Li-redox-active lithium iron phosphate (LFP) has excellent thermal and electrochemical stability as well as Li-redox activity at relatively high voltages, and it can be uniformly coated on the NCA surface by an industrially feasible melt mixing and calcination process. This reduces the side reaction between the NCA and the electrolyte and the degree of disorder of the cations in NCA [67]. Chen et al. [68] showed that the capacity of the full cell prepared by this simple method of NCA-LFP material was greatly improved at high temperature and higher charging voltage. After 100 charge and discharge cycles, NCA-LFP exhibited an excellent capacity retention of 95% at high charging voltage (4.5 V) and high temperature (55°C), which is 15% higher than in the original NCA cathode. This improvement in electrochemical performance and thermal stability at high voltages is attributed to the reduction in the degree of cation mixing in the NCA and the reduction in SEI film formation in the presence of the LFP coating, as shown in Figure 3.

2.5. Fluoride Coating. Fluoride is also one of the most widely used materials in the coating modification of lithium-ion battery cathode materials. A key factor in the electrochemical performance degradation of lithium-ion batteries is that

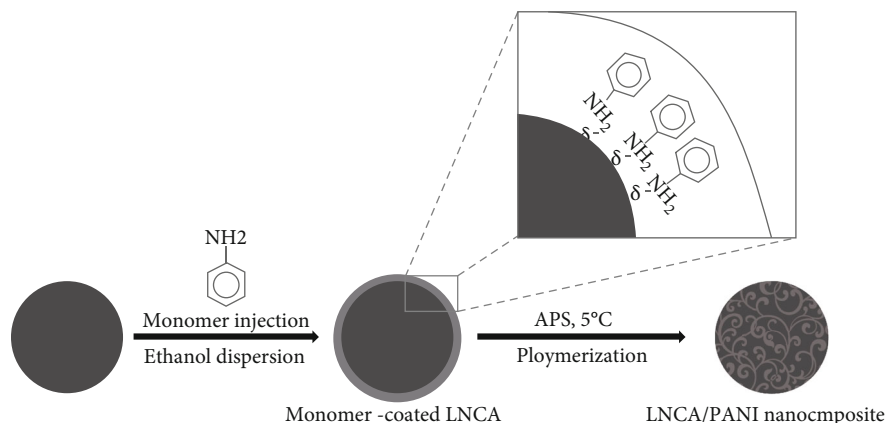


FIGURE 4: A scheme illustrating the LNCA material surface coated by polyaniline [80].

electrolyte LiPF_6 will decompose continuously during battery operation to produce highly corrosive hydrofluoric acid (HF), which causes the dissolution of transition metals in NCA cathode materials. The decomposition of LiPF_6 generates LiF and PF_5 . The LiF is deposited on the surface of the active material, and it has a low Li^+ and electron permeability. Meanwhile, the PF_5 reacts with the trace amount of water in the electrolyte to form HF, which causes corrosion to the electrode material and further enhances the instability of the interface between electrode and electrolyte. Therefore, an important method to increase the capacity retention of lithium-ion batteries is to slow the dissolution of transition metals in the active materials. Fluoride-coated positive electrode materials are directly used in lithium-ion batteries. On the one hand, the common electrolyte for lithium-ion batteries is LiPF_6 , and F^- can effectively suppress the occurrence of interfacial reactions [69]. On the other hand, the addition of F can lower the charge transfer resistance and improve the conductivity, thereby improving the rate performance and cycle performance of the cathode material [70].

The fluorides currently used for coating include AlF_3 , MgF_2 , CaF_2 , YF_3 , LaF_3 , GaF_3 , and LiF [71–75]. Lee et al. [76] mixed the homemade AlF_3 with NCA and obtained the NCA/AlF_3 material after high-speed ball milling (3400 r/min) for 5 min. The cycle performance rate performance and thermal stability of the coated material were improved, especially at high temperatures. Tested at 55°C and 1.0 C, the capacity retention of NCA/AlF_3 material after 500 cycles was 55.9%, much higher than the 11.7% for the raw materials. On the one hand, the coating inhibits the erosion of the HF electrode material, reduces the dissolution of the transition metal in the electrolyte, and thus reduces the growth of charge transfer resistance. On the other hand, the coating reduces the volume change of the material, thereby preventing the material from chalking during the cycle. Fluoride has a high electronegativity and forms a stable compound with 3D transition metal elements [77]. Furthermore, the mixture has desirable thermal stability at elevated temperatures for lithium-ion batteries. Liu et al. [78] used a solvating-out crystallization process to coat a 10–20 nm thick FeF_3 layer on NCA. The electrochemical properties of the battery significantly improved, where the

discharge capacity of bare NCA decreased sharply from 180.9 to 81.8 mAh g^{-1} , with a retention of 45.2% after 100 cycles at 1.0 C and 55°C , while the discharge capacity of FeF_3 -coated NCA decreased from 182.2 to 105.4 mAh g^{-1} , with a retention of 57.8%. When the cycle number increased from 2 to 50, the charge transfer resistance value of bare NCA increased from 64Ω to 218Ω , but that of coated NCA increased only from 58Ω to 166Ω . This indicates that the FeF_3 coating reduced the side reactions between the cathode and electrolyte, thus suppressing the impedance increase. The reason can be mainly attributed to the FeF_3 coating effectively improving the electrochemical properties of NCA, including the rate capability, cycle performance, and high-temperature property.

2.6. Polymer Coating. Some polymers have good electrical conductivity and can be used for the surface coating of NCA materials. In addition, the conductive polymer has a certain blocking effect of preventing intergranular cracking of the NCA particles. Among the conducting polymers, polyaniline (PANI) is popular due to its ease of coating, simple preparation, environmental stability, and low cost. NCA/PANI materials were prepared by Chung and Ryu [79] using in situ self-stabilizing dispersion polymerization to coat a layer of polyaniline on the surface of NCA material as shown in Figure 4. The synthesized NCA/PANI has a similar particle size to NCA and demonstrated good cycling performance compared with pristine NCA to 40 cycles. PANI (the emeraldine salt form) provides good contact between polymer and oxide particles, resulting in the observed increase in the electrical conductivity of the composite compared with the pristine NCA. Moreover, this material showed good reversibility for Li insertion in discharge cycles when used as the electrode of lithium-ion batteries. Poly(3-hexylthiophene-2,5-diyl) (P3HT), a conducting polymer studied extensively for its optoelectronic devices, offers several advantageous properties when used as a cladding material for lithium-ion battery cathode materials. Lai et al. [80] prepared P3HT for both surface protection and as a conductive layer for NCA. The thickness was carefully controlled to limit the ionic resistance while providing sufficient electronic conduction. The improved conduction

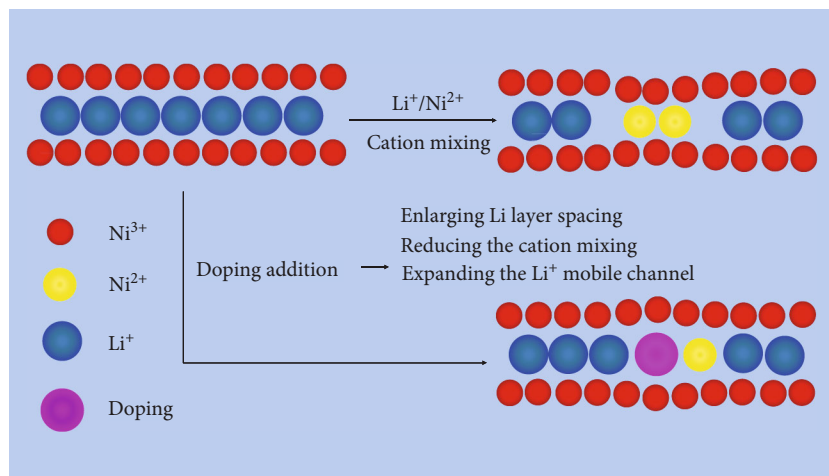


FIGURE 5: Possible function mechanism of doping in NCA [81].

enables higher power densities to be attained compared with the control NCA electrodes, which were made with the standard binder polymer. The dense P3HT coating provides limited spacing for ion transport of the bulky reactants generated from the electrolyte breakdown. In this way, the P3HT functions as an artificial SEI, protecting the NCA from degradation. The integration of P3HT with NCA enables the resulting material to perform as a high rate positive electrode for lithium-ion batteries. Moreover, the use of the P3HT-CNT binder system led to improved cycling for NCA at high power density with capacities of 80 mAh g^{-1} obtained after 1000 cycles at 16.0 C, a value that was 4 times greater than that achieved in the control electrode.

3. Doping and Functionalization

Unlike the surface coating, the problem of NCA is solved from the surface of the material, whereas the bulk phase is focused on improving the performance from the internal structure of the material. Primarily, the use of additional atomic doping combines the properties of foreign atoms with NCA to enhance the features of NCA or overcome the shortcomings of NCA. At present, there are two kinds of doping modifications for NCA cathode materials: cationic doping and anionic doping. Successful doping does not affect the structure of NCA-positive electrode materials, nor does it form impurities. Doping can also inhibit Ni²⁺ from occupying Li⁺ vacancies, which reduces the phenomenon of cation mixing and increases the unit cell parameter c , reduces the irreversible capacity loss during charge and discharge, and improves the electrochemical performance of the material. The possible doping mechanism is shown in Figure 5.

3.1. Cationic Doping. Further research with alternative transition metal elements will help to optimize the structural design of the NCA-based materials to balance the specific capacity, cycle performance, and electrical conductivity of the materials. Mn and Ti have atomic radii similar to Ni and coordinate with oxygen to replace transition metal atoms

in octahedral interstitial sites. Wan et al. [82] prepared a $\text{LiNi}_{0.85}\text{Co}_{0.1}\text{Al}_{0.05}\text{O}_2$ (NCA) cathode material by hydrothermal reaction and doping with the transition metals Mn and Ti, respectively. In the voltage range of 3.0–4.3 V, the initial discharge specific capacity of NCA-Ti and NCA-Mn was 179.6 mAh g^{-1} and 171.4 mAh g^{-1} , respectively, which was higher than that of undoped NCA (156.5 mAh g^{-1}). The octahedral lattice space occupied by lithium ions introduced by Mn⁴⁺ and Ti⁴⁺ increases the unit cell volume and enlarges the lithium layer spacing, thereby improving the diffusion of lithium ions and thus improving the electrochemical performance of the cathode material. Moreover, the SEI film resistance (R_1) values of the LIBs with the fresh NCA, NCA-Mn, and NCA-Ti electrodes were 31.1, 52.4, and 24.2Ω , respectively. The smallest R_1 of the NCA-Ti electrode suggests that the NCA-Ti electrode has better electrochemical properties and abilities for rapid electron transport during the electrochemical Li⁺ insertion/extraction reaction. Titanium ions with a large ionic radius can modify the oxygen crystal lattice, improve the local coordination environment of NCA, reduce the cation mixing, and make the material have better kinetics and thermodynamic properties and structural stability. Qiu et al. [83] demonstrated that the appropriate amount of Ti substitution could enable the NCA cathode to be operated with a high cut-off voltage. The XRD and TEM results showed Ti doping can effectively inhibit the mixing of Li⁺/Ni²⁺ and the surface of the NiO phase on the surface of NCA kinetics and thermodynamics. At a high cut-off voltage of 4.7 V, 1% Ti-doped NCA (NCAT-1) had the highest reversible capacity of 198 mAh g^{-1} at 0.1 C, and its capacity retention after 100 cycles was 86.9%. In addition, NCAT-1 has a lower Li⁺ diffusion coefficient and rate performance with higher voltage polarizability than NCA cathodes. The FeO₆ octahedron formed in the Fe-doped NCA material affects the edge-shared NiO₆ octahedron, which enhances electron localization, reduces the tendency to generate active oxygen species at the interface, inhibits oxidation of the electrolyte, and stabilizes the interface [84]. $\text{LiNi}_{0.8}\text{Co}_{0.15-y}\text{Fe}_y\text{Al}_{0.05}\text{O}_2$ (NCFA, $0 \leq y \leq$

TABLE 1: Crystallographic formula of the prepared samples before and after 10 cycles based on the ICP-AES results [92].

Samples	Crystallographic formula	
	Before cycling	After 10 cycles
NCA	$\text{Li}_{1.004}\text{Ni}_{0.803}\text{Co}_{0.147}\text{Al}_{0.046}\text{O}_2$	$\text{Li}_{0.994}\text{Ni}_{0.809}\text{Co}_{0.149}\text{Al}_{0.048}\text{O}_2$
NNCA	$\text{Li}_{1.002}\text{Na}_{0.009}\text{Ni}_{0.798}\text{Co}_{0.146}\text{Al}_{0.045}\text{O}_2$	$\text{Li}_{0.999}\text{Na}_{0.003}\text{Ni}_{0.802}\text{Co}_{0.149}\text{Al}_{0.047}\text{O}_2$
KNCA	$\text{Li}_{0.999}\text{K}_{0.008}\text{Ni}_{0.797}\text{Co}_{0.147}\text{Al}_{0.049}\text{O}_2$	$\text{Li}_{0.997}\text{K}_{0.008}\text{Ni}_{0.798}\text{Co}_{0.148}\text{Al}_{0.049}\text{O}_2$

0.15) cathode materials were systematically studied by Du et al. [85] using ball milling from the mixture of $\text{Ni}(\text{OH})_2$, Co_3O_4 , Al_2O_3 , Fe_2O_3 , and Li_2CO_3 under alcohol media for 8 h and then calcinated under flowing oxygen at 720°C for 8 h. The characterization results show that the assembled battery can present excellent physicochemical and battery performance when the Fe substitution is 0.075, the discharge capacity of NCA can reach 167.2 mAh g^{-1} (NCA is 183.9 mAh g^{-1}), and the cycle performance is excellent. In addition, the capacity retention rate was 88.4% after 350 cycles (55.7% for NCA) due to the suppression of phase transitions and stable electrode-electrolyte interface. As the iron content increases, the (003) and (104) peaks move toward small angles, and these diffraction peaks are particularly sensitive to changes in the c -axis and the a -axis of the hexagonal unit cell [86, 87]. The refinement of the XRD pattern by the Rietveld method using GSAS software confirmed that the substitution of Fe might lead to an increase in c -axis and a -axis values. The increase in the a value and c value is probably because the ionic radius of Fe^{3+} (0.645 \AA) is greater than Co^{3+} (0.545 \AA). However, the c/a ratios of the two samples were similar, indicating that no disordered phase was formed in the presence of an appropriate amount of iron [88], indicating that NCA still has an excellent lamellar structure.

Excessive element doping is an effective method to improve the structural stability of layered cathode oxides [89], and elements doped at the Li site have also proven to be a viable method to prevent the collapse of layered structures. Na-doped samples have good oxidation resistance, lower potential polarization, higher initial coulomb efficiency, better rate performance, and so on. These characteristics can also be detected and elaborated in the references. For example, Wang et al. [88] doped 1% (by weight) NaCl into $\text{LiNi}_{0.8}\text{Co}_{0.15}\text{Al}_{0.05}\text{O}_2$; the obtained Na-doped sample had superior cycle stability at 1.0 C, where the initial discharge specific capacity of the original NCA and the doped NCA did not differ significantly, 182.9 mAh g^{-1} and 183.9 mAh g^{-1} , respectively. After 300 cycles, the capacity of the doped NCA sample remained 81.6%, higher than in the original NCA (48.1%); by the columnar effect of the large radius of Na^+ , the Na-doped NCA sample particles retained a complete spherical morphology even after many cycles. The incorporation of a large radius of alkali ions can increase the lithium layer spacing and reduce the degree of cation mixing by increasing the diffusivity of Li^+ in the bulk structure. In addition, potassium has similar chemistry to sodium and a larger ionic radius (1.38 \AA) and lower electronegativity [90, 91]. Zhao et al. [92] anchored 1% K^+ to the Li^+ site of $\text{LiNi}_{0.8}\text{Co}_{0.15}\text{Al}_{0.05}\text{O}_2$ as an excellent structural stabilizer compared with the Na^+ -doping material

with a similarity to the original material and modification mechanism, and the K^+ -doped cathode material exhibited higher initial coulombic efficiency and better rate performance; $\text{Li}_{0.99}\text{K}_{0.01}\text{Ni}_{0.8}\text{Co}_{0.15}\text{Al}_{0.05}\text{O}_2$ had a large initial discharge capacity of 216.8 mAh g^{-1} at 0.1 C and maintained 87.4% after 150 cycles of a stable cycle at 4.6 V high voltage and 1.0 C. The ICP-AES results are shown in Table 1. Moreover, Na^+ can migrate from the material to the electrolyte during the high-pressure cycle, and the migration of Na^+ causes the material to also undergo severe capacity decay. In contrast, K^+ with a larger ionic radius and lower migration ability can stabilize and inhibit the irreversible phase transition between H2 and H3 and the degradation of the host structure by occupying the lithium layer firmly. At the same time, K^+ in the Li^+ site prevents the formation of trivacancies in the highly delithiated state by alleviating the cation migration and the generation of the resistive spinel and rock salt phases during the high-pressure cycle, as shown in Figure 6. Considering the enhanced structural stability of the Ni-rich cathode material by K^+ anchoring under high-pressure cycling, it provides an extraordinary hint for the rational design of advanced cathode materials for the pursuit of high-energy density lithium-ion batteries.

3.2. Anionic Doping. Another method to improve the cycling stability of lithium-ion battery electrode materials is anion doping. The negative ions currently used are F^- [93, 94], Cl^- [95, 96], Br^- [97, 98], S^{2-} [99], PO_4^{3-} [100], and so on. In recent years, to improve the performance of NCA, F^- has been added to the list of anions deployed by cryogenic methods. F^- doping indicates that the process is a catalyst that promotes the growth of primary particles. The valence state of the surface nickel ions decreases, the spacing between the plates increases, and the increase in the impedance during the cycle is reduced, which is beneficial to inhibiting the degradation of NCA material. Huang et al. [94] prepared different amounts of NH_4F and NCA dispersed in anhydrous ethanol, and the mixture was continuously evaporated and dried. It was homogeneous and calcined in air at 420°C for 4 h to obtain an F-doped NCA material (NCAF). As the concentration of fluorine increased, some of the nickel ions were reduced, resulting in a decrease in the initial discharge capacity. NCAF had the best electrochemical performance when NH_4F was added at 2 mol %, and the cycle performance of NCAF was improved at room temperature, high temperature (55°C), and high cut-off potential (4.5 V).

In contrast, NCA modified with Br will have a more stable structure than N modified with F, and the electron affinity of Br is greater than O and F (Br: $342.54\text{ kJ mol}^{-1}$, F:

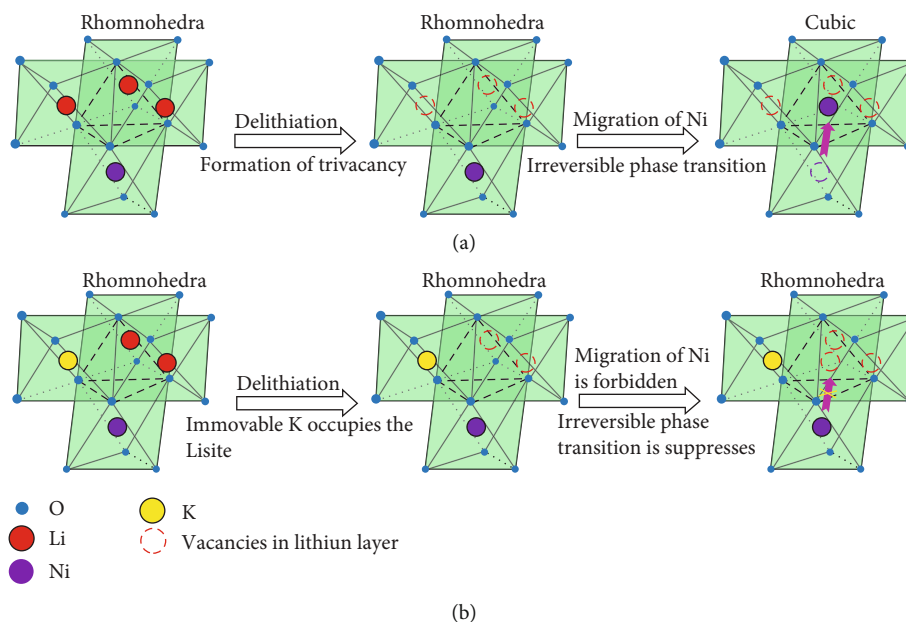


FIGURE 6: Schematic diagrams of the phase evolution routes for (a) potassium-free and (b) potassium-doped samples, which are built on an O_3 -layered model with unrealistic radius ratios [92].

328.1 kJ mol⁻¹, and O: 141.3 kJ mol⁻¹), so M- (Ni, Co, Al) Br is stronger than the M- (Ni, Co, Al) O or M- (Ni, Co, Al) F bond. In addition, Br⁻ doping is expected to produce an NCA similar to the F⁻-doping mechanism. Furthermore, the ionic radius (0.196 nm) of Br⁻ is larger than F⁻ (0.133 nm) or O²⁻ (0.140 nm), and the NCA modified with Br⁻ may increase the Li⁺ mobility. He et al. [101] modified the electrochemical properties of LiNi_{0.815}Co_{0.15}Al_{0.035}O₂ (NCA) cathode material by in situ Br⁻ doping. The effects of Br⁻ modification on the structure, morphology, and electrochemical properties of NCA cathode materials were systematically investigated. The results of structural characterization show that part of the Br⁻ doped into the bulk particles of NCA replaces O²⁻ at position 6c, thus forming a strong bond between the metal and Br⁻ by stabilizing the main structure and improving the stability of NCA against HF attack. At the same time, the gap spacing of the NCA is increased, and the growth of the primary particles is suppressed by the Br⁻ modification, providing a wider channel and a shorter path for Li⁺. In addition, due to the incorporation of Br⁻, the Ni³⁺ portion of the surface is reduced to Ni²⁺, which also contributes to improving the structural stability of the NCA. The residual lithium acts as a stable LiBr rather than an unstable Li₂CO₃, which can suppress the reductive decomposition reaction of the electrolyte. Electrochemical tests show that 0.2 mol% Br⁻-doped NCA (NCABr-2) reduces potential polarization, decreasing the $R_{sf} + R_{ct}$ value and increasing the Li⁺ diffusion coefficient. The capacity retention rate of NCABr-2 was 73.7% after circulating for 100 cycles at 0.5 C, which was higher than the 63.7% of the original NCA material. Moreover, Br⁻ doping can effectively improve the cycle performance of the NCA cathode material, and this performance is more obvious at high temperatures. The cycle retention of NCABr-2 at 55°C and 0.5 C was 75.7%, which was much higher than the 41.5% of pure

NCA material. These results clearly show that Br⁻ doping contributes significantly to the structural stability and cycle performance of the NCA material.

Chen et al. [102] adopted a gradient boron-polyanion-doped nickel-rich LiNi_{0.8}Co_{0.15}Al_{0.05}O₂ cathode material. When the doping amount was 1.5% (molar percentage), the sample B0.015-NCA had the best cycle performance. It also worked well at high voltage (4.5 V) and high temperature (55°C). The SEM images analyzed the presence of cracks and thicker SEI layers on the elementary particles after 100 cycles at high temperature while the doped particles were intact and the SEI layer was thinner, which reduced the capacity/potential decay during charge and discharge. Electrochemical impedance spectroscopy confirmed that boron-polyanion doping could suppress the increase in impedance during high-temperature cycling. The advantages of gradient polyanion doping in a structure are mainly reflected in two aspects. On the one hand, the outer layer of boron-rich polyanion decreases the average valence of nickel ions and reduces the surface reaction of the material. The activity inhibits the decomposition of the organic electrolyte and plays a role in surface modification. On the other hand, due to the reduction of the Ni-O covalent bond and the introduction of the B-O covalent bond with high bond energy, the change in the 2p orbital of the O atom and the formation of cracks are effectively alleviated in the charge and discharge process.

4. Conclusions

Given that the NCA material is expected to become the future cathode material of the lithium-ion battery, it is necessary to pay attention to the practicability of materials. The modification methods of materials should also be designed with practicability in mind. It is essential to consider the

compatibility of the coated or doped NCA material with the electrolyte and the negative electrode material, compatibility with the battery manufacturing process, and adaptability. For the needs of large-scale production, the experimental conditions of the modification process should be as simple as possible, avoiding the use of more energy-intensive methods and saving costs. In addition, it is better to use modified materials that are relatively easy to obtain with a wide range of sources, which is conducive to the large-scale application of NCA materials and to meeting the demand for battery materials in various fields of society in the future. Moreover, the design of the material itself is also one of the methods to solve the current problem, and the coating and doping technology is more important for the modification of NCA materials with higher Ni content in terms of capacity and price.

Conflicts of Interest

The authors declare that they have no conflicts of interest.

Acknowledgments

This work was financially supported by the National Natural Science Foundation of China (Nos. 51874046 and 51404038), the Project of Scientific Research of Jingzhou (No. 2018029), and the Yangtze Youth Talents Fund (No. 2016cqr05).

References

- [1] B. Scrosati and J. Garche, "Lithium batteries: status, prospects and future," *Journal of Power Sources*, vol. 195, no. 9, pp. 2419–2430, 2010.
- [2] M. Bini, D. Capsoni, S. Ferrari, E. Quartarone, and P. Mustarelli, "Rechargeable lithium batteries: key scientific and technological challenges," *Rechargeable Lithium Batteries*, vol. 195, no. 9, pp. 1–17, 2015.
- [3] G. E. Blomgren, "The development and future of lithium ion batteries," *Journal of the Electrochemical Society*, vol. 164, no. 1, pp. A5019–A5025, 2017.
- [4] N. Nitta, F. Wu, J. T. Lee, and G. Yushin, "Li-ion battery materials: present and future," *Materials Today*, vol. 18, no. 5, pp. 252–264, 2015.
- [5] F. Cheng, J. Liang, Z. Tao, and J. Chen, "Functional materials for rechargeable batteries," *Advanced Materials*, vol. 23, no. 15, pp. 1695–1715, 2011.
- [6] K. Ozawa, "Lithium-ion rechargeable batteries with LiCoO₂ and carbon electrodes: the LiCoO₂/C system," *Solid State Ionics*, vol. 69, no. 3-4, pp. 212–221, 1994.
- [7] T. F. Yi, P. P. Peng, X. Han, Y. R. Zhu, and S. Luo, "Interconnected Co₃O₄@CoNiO₂@PPy nanorod and nanosheet composite grown on nickel foam as binder-free electrodes for Li-ion batteries," *Solid State Ionics*, vol. 329, pp. 131–139, 2019.
- [8] T. Ohzuku, A. Ueda, M. Nagayama, Y. Iwakoshi, and H. Komori, "Comparative study of LiCoO₂, LiNi₁₂Co₁₂O₂ and LiNiO₂ for 4 volt secondary lithium cells," *Electrochimica Acta*, vol. 38, no. 9, pp. 1159–1167, 1993.
- [9] T. Ohzuku, A. Ueda, and M. Nagayama, "Electrochemistry and Structural Chemistry of LiNiO₂ (R3m) for 4 Volt Secondary Lithium Cells," *Journal of the Electrochemical Society*, vol. 140, no. 7, pp. 1862–1870, 1993.
- [10] E. Zhecheva and R. Stoyanova, "Stabilization of the layered crystal structure of LiNiO₂ by co-substitution," *Solid State Ionics*, vol. 66, no. 1-2, pp. 143–149, 1993.
- [11] E. Levi, M. D. Levi, G. Salitra et al., "Electrochemical and in-situ XRD characterization of LiNiO₂ and LiCo_{0.2}Ni_{0.8}O₂ electrodes for rechargeable lithium cells," *Solid State Ionics*, vol. 126, no. 1-2, pp. 97–108, 1999.
- [12] K. Zhu, T. Wu, Y. Zhu et al., "Layered Fe-substituted LiNiO₂ Electrochemicals for high-efficiency oxygen evolution reaction," *ACS Energy Letters*, vol. 2, no. 7, pp. 1654–1660, 2017.
- [13] M. Song, I. Kwon, S. Shim, and J. H. Song, "Electrochemical characterizations of Fe-substituted LiNiO₂ synthesized in air by the combustion method," *Ceramics International*, vol. 36, no. 4, pp. 1225–1231, 2010.
- [14] M. K. Majee, A. K. Nigam, and P. A. Bhoobe, "Comparison of local crystal structure and magnetic properties of cation substituted LiNiO₂ compositions," *Materials Research Bulletin*, vol. 116, pp. 143–152, 2019.
- [15] Z. Qiu, Y. Zhang, X. Huang et al., "Beneficial effect of incorporating Ni-rich oxide and layered over-lithiated oxide into high-energy-density cathode materials for lithium-ion batteries," *Journal of Power Sources*, vol. 400, pp. 341–349, 2018.
- [16] H. S. Ko, J. H. Kim, J. Wang, and J. D. Lee, "Co/Ti co-substituted layered LiNiO₂ prepared using a concentration gradient method as an effective cathode material for Li-ion batteries," *Journal of Power Sources*, vol. 372, pp. 107–115, 2017.
- [17] C. S. Yoon, U. H. Kim, G. T. Park et al., "Self-passivation of a LiNiO₂ Cathode for a lithium-ion battery through Zr doping," *ACS Energy Letters*, vol. 3, no. 7, pp. 1634–1639, 2018.
- [18] H. Ouyang, X. Li, Z. Wang, H. Guo, and W. Peng, "Electrochemical and structural analysis of Mg substitution in lithium-rich layered oxide for lithium-ion battery," *Ionics*, vol. 24, no. 11, pp. 3347–3356, 2018.
- [19] Z. Y. Li, H. Guo, X. Ma et al., "Al substitution induced differences in materials structure and electrochemical performance of Ni-rich layered cathodes for lithium-ion batteries," *The Journal of Physical Chemistry C*, vol. 123, no. 32, pp. 19298–19306, 2019.
- [20] M. S. Whittingham, "Ultimate limits to intercalation reactions for lithium batteries," *Chemical Reviews*, vol. 114, no. 23, pp. 11414–11443, 2014.
- [21] S. Xia, F. Li, F. Cheng et al., "Synthesis of spherical fluorine modified gradient Li-ion battery cathode material LiNi_{0.80}Co_{0.15}Al_{0.05}O₂ by simple solid phase method," *Journal of the Electrochemical Society*, vol. 165, no. 5, pp. A1019–A1026, 2018.
- [22] W. Chen, Y. Li, D. Yang, X. Feng, X. Guan, and L. Mi, "Controlled synthesis of spherical hierarchical LiNi_{1-x-y}Co_xAl_yO₂ (0 < x, y < 0.2) via a novel cation exchange process as cathode materials for high-performance lithium batteries," *Electrochimica Acta*, vol. 190, pp. 932–938, 2016.
- [23] J. Duan, P. Dong, D. Wang et al., "A facile structure design of LiNi_{0.90}Co_{0.07}Al_{0.03}O₂ as advanced cathode materials for lithium ion batteries via carbonation decomposition of NaAl(OH)₄ solution," *Journal of Alloys and Compounds*, vol. 739, pp. 335–344, 2018.
- [24] N. M. Trease, I. D. Seymour, M. D. Radin et al., "Identifying the distribution of Al³⁺ in LiNi_{0.8}Co_{0.15}Al_{0.05}O₂," *Chemistry of Materials*, vol. 28, no. 22, pp. 8170–8180, 2016.

- [25] K. J. Park, J. Y. Hwang, H. H. Ryu et al., "Degradation mechanism of Ni-enriched NCA cathode for lithium batteries: are microcracks really critical?," *ACS Energy Letters*, vol. 4, no. 6, pp. 1394–1400, 2019.
- [26] H. Chen, J. A. Dawson, and J. H. Harding, "Effects of cationic substitution on structural defects in layered cathode materials LiNiO_2 ," *Journal of Materials Chemistry A*, vol. 2, no. 21, pp. 7988–7996, 2014.
- [27] J. Y. Liao and A. Manthiram, "Surface-modified concentration-gradient Ni-rich layered oxide cathodes for high-energy lithium-ion batteries," *Journal of Power Sources*, vol. 282, pp. 429–436, 2015.
- [28] I. Hwang, C. W. Lee, J. C. Kim, and S. Yoon, "Particle size effect of Ni-rich cathode materials on lithium ion battery performance," *Materials Research Bulletin*, vol. 47, no. 1, pp. 73–78, 2012.
- [29] F. Wu, J. Tian, Y. Su et al., "Effect of Ni^{2+} content on lithium/nickel disorder for Ni-rich cathode materials," *ACS Applied Materials & Interfaces*, vol. 7, no. 14, pp. 7702–7708, 2015.
- [30] T. Nonaka, C. Okuda, Y. Seno, H. Nakano, K. Koumoto, and Y. Ukyo, "In situ XAFS and micro-XAFS studies on $\text{LiNi}_{0.8}\text{Co}_{0.15}\text{Al}_{0.05}\text{O}_2$ cathode material for lithium-ion batteries," *Journal of Power Sources*, vol. 162, no. 2, pp. 1329–1335, 2006.
- [31] W. Liu, P. Oh, X. Liu, S. Myeong, W. Cho, and J. Cho, "Countering voltage decay and capacity fading of lithium-rich cathode material at 60 °C by hybrid surface protection layers," *Advanced Energy Materials*, vol. 5, no. 13, pp. 1500274–1500284, 2015.
- [32] T. Nonaka, C. Okuda, Y. Seno, K. Koumoto, and Y. Ukyo, "X-ray absorption study on $\text{LiNi}_{0.8}\text{Co}_{0.15}\text{Al}_{0.05}\text{O}_2$ cathode material for lithium-ion batteries," *Ceramics International*, vol. 34, no. 4, pp. 859–862, 2008.
- [33] G. V. Zhuang, G. Chen, J. Shim, X. Song, P. N. Ross, and T. J. Richardson, " Li_2CO_3 in $\text{LiNi}_{0.8}\text{Co}_{0.15}\text{Al}_{0.05}\text{O}_2$ cathodes and its effects on capacity and power," *Journal of Power Sources*, vol. 134, no. 2, pp. 293–297, 2004.
- [34] W. L. Ong, S. M. Rupich, D. V. Talapin, A. J. H. McGaughey, and J. A. Malen, "Surface chemistry mediates thermal transport in three-dimensional nanocrystal arrays," *Nature Materials*, vol. 12, no. 5, pp. 410–415, 2013.
- [35] D. Mohanty, K. Dahlberg, D. M. King et al., "Modification of Ni-rich FCG NMC and NCA cathodes by atomic layer deposition: preventing surface phase transitions for high-voltage lithium-ion batteries," *Scientific Reports*, vol. 6, no. 1, pp. 26532–26537, 2016.
- [36] T. F. Yi, P. P. Peng, Z. Fang, Y. R. Zhu, Y. Xie, and S. Luo, "Carbon-coated $\text{LiMn}_{1-x}\text{Fe}_x\text{PO}_4$ ($0 \leq x \leq 0.5$) nanocomposites as high-performance cathode materials for Li-ion battery," *Composites Part B: Engineering*, vol. 175, pp. 107067–107076, 2019.
- [37] S. Yoon, K. N. Jung, S. H. Yeon, C. S. Jin, and K. H. Shin, "Electrochemical properties of $\text{LiNi}_{0.8}\text{Co}_{0.15}\text{Al}_{0.05}\text{O}_2$ -graphene composite as cathode materials for lithium-ion batteries," *Journal of Electroanalytical Chemistry*, vol. 683, pp. 88–93, 2012.
- [38] Z. Jiang, Y. Li, J. Zhu et al., "Synthesis and performance of a graphene decorated $\text{NaTi}_2(\text{PO}_4)_3/\text{C}$ anode for aqueous lithium-ion batteries," *Journal of Alloys and Compounds*, vol. 791, pp. 176–183, 2019.
- [39] R. Fang, C. Miao, H. Mou, and W. Xiao, "Facile synthesis of ₂/rGO composite with sandwich-like nanostructure as superior performance anodes for lithium ion batteries," *Journal of Alloys and Compounds*, pp. 152884–152891, 2019.
- [40] Y. M. Chung, S. H. Ryu, J. H. Ju et al., "A surfactant-based method for carbon coating of $\text{LiNi}_{0.8}\text{Co}_{0.15}\text{Al}_{0.05}\text{O}_2$ Cathode in Li ion batteries," *Bulletin of the Korean Chemical Society*, vol. 31, no. 8, pp. 2304–2308, 2010.
- [41] Z. Liu, Z. Wang, T. Lu, P. Dai, P. Gao, and Y. Zhu, "Modification of $\text{LiNi}_{0.8}\text{Co}_{0.15}\text{Al}_{0.05}\text{O}_2$ using nanoscale carbon coating," *Journal of Alloys and Compounds*, vol. 763, pp. 701–710, 2018.
- [42] X. Wang, L. Lv, Z. Cheng et al., "High-density monolith of N-doped holey graphene for ultrahigh volumetric capacity of Li-ion batteries," *Advanced Energy Materials*, vol. 6, no. 6, pp. 1502100–1502106, 2016.
- [43] C. Li, B. Xie, Z. He, J. Chen, and Y. Long, "3D structure fungi-derived carbon stabilized stearic acid as a composite phase change material for thermal energy storage," *Renewable Energy*, vol. 140, pp. 862–873, 2019.
- [44] X. He, G. Han, S. Lou et al., "Improved electrochemical performance of $\text{LiNi}_{0.8}\text{Co}_{0.15}\text{Al}_{0.05}\text{O}_2$ Cathode material by coating of graphene nanodots," *Journal of the Electrochemical Society*, vol. 166, no. 6, pp. A1038–A1044, 2019.
- [45] P. Gao, Y. Jiang, Y. Zhu, and H. Hu, "Improved cycle performance of nitrogen and phosphorus co-doped carbon coatings on lithium nickel cobalt aluminum oxide battery material," *Journal of Materials Science*, vol. 53, no. 13, pp. 9662–9673, 2018.
- [46] R. Fang, W. Xiao, C. Miao et al., "Enhanced lithium storage performance of core-shell structural $\text{Si}@\text{TiO}_2/\text{NC}$ composite anode via facile sol-gel and *in situ* N-doped carbon coating processes," *Electrochimica Acta*, vol. 317, pp. 575–582, 2019.
- [47] Z. Wang, C. Miao, W. Xiao et al., "Effect of different contents of organic-inorganic hybrid particles poly(methyl methacrylate)- ZrO_2 on the properties of poly(vinylidene fluoride-hexafluoropropylene)-based composite gel polymer electrolytes," *Electrochimica Acta*, vol. 272, pp. 127–134, 2018.
- [48] W. Xiao, Z. Wang, Y. Zhang et al., "Enhanced performance of P(VDF-HFP)-based composite polymer electrolytes doped with organic-inorganic hybrid particles PMMA- ZrO_2 for lithium ion batteries," *Journal of Power Sources*, vol. 382, pp. 128–134, 2018.
- [49] Z. Xie, Y. Zhang, A. Yuan, and J. Xu, "Effects of lithium excess and SnO_2 surface coating on the electrochemical performance of $\text{LiNi}_{0.8}\text{Co}_{0.15}\text{Al}_{0.05}\text{O}_2$ cathode material for Li-ion batteries," *Journal of Alloys and Compounds*, vol. 787, pp. 429–439, 2019.
- [50] R. Li, C. Miao, M. Zhang, and W. Xiao, "Novel hierarchical structural SnS_2 composite supported by biochar carbonized from chewed sugarcane as enhanced anodes for lithium ion batteries," *Ionics*, pp. 1–9, 2019.
- [51] B. S. Liu, X. L. Sui, S. H. Zhang et al., "Investigation on electrochemical performance of $\text{LiNi}_{0.8}\text{Co}_{0.15}\text{Al}_{0.05}\text{O}_2$ coated by heterogeneous layer of TiO_2 ," *Journal of Alloys and Compounds*, vol. 739, pp. 961–971, 2018.
- [52] R. Li, W. Xiao, C. Miao, R. Fang, Z. Wang, and M. Zhang, "Sphere-like $\text{SnO}_2/\text{TiO}_2$ composites as high-performance anodes for lithium ion batteries," *Ceramics International*, vol. 45, no. 10, pp. 13530–13535, 2019.

- [53] X. He, C. Du, B. Shen et al., “Electronically conductive Sb-doped SnO₂ nanoparticles coated LiNi_{0.8}Co_{0.15}Al_{0.05}O₂ cathode material with enhanced electrochemical properties for Li-ion batteries,” *Electrochimica Acta*, vol. 236, pp. 273–279, 2017.
- [54] J. C. Zheng, Z. Yang, Z. J. He, H. Tong, W. J. Yu, and J. F. Zhang, “In situ formed LiNi_{0.8}Co_{0.15}Al_{0.05}O₂@Li₄SiO₄ composite cathode material with high rate capability and long cycling stability for lithium-ion batteries,” *Nano Energy*, vol. 53, pp. 613–621, 2018.
- [55] R. Qi, J. L. Shi, X. D. Zhang et al., “Improving the stability of LiNi_{0.80}Co_{0.15}Al_{0.05}O₂ by AlPO₄ nanocoating for lithium-ion batteries,” *Science China Chemistry*, vol. 60, no. 9, pp. 1230–1235, 2017.
- [56] X. Zhang, G. Liu, S. Li, H. Dong, H. Liu, and J. Mei, “Preparation of a homogeneous Li₃PO₄ coating and its effect on the electrochemical properties of LiNi_{0.8}Co_{0.15}Al_{0.05}O₂,” *Journal of Electronic Materials*, vol. 48, no. 7, pp. 4443–4451, 2019.
- [57] Z. Wang, Z. Kou, C. Miao, and W. Xiao, “Improved performance all-solid-state electrolytes with high compacted density of monodispersed spherical Li_{1.3}Al_{0.3}Ti_{1.7}(PO₄)₃ particles,” *Ceramics International*, vol. 45, no. 11, pp. 14469–14473, 2019.
- [58] D. J. Lee, B. Scrosati, and Y. K. Sun, “Ni₃(PO₄)₂-coated Li[Ni_{0.8}Co_{0.15}Al_{0.05}]O₂ lithium battery electrode with improved cycling performance at 55 °C,” *Journal of Power Sources*, vol. 196, no. 18, pp. 7742–7746, 2011.
- [59] Y. R. Bak, Y. Chung, J. H. Ju, M. J. Hwang, Y. Lee, and K. S. Ryu, “Structure and Electrochemical Performance of LiNi_{0.8}Co_{0.15}Al_{0.05}O₂ Cathodes Before and After Treatment with Co₃(PO₄)₂ or AlPO₄ by *in situ* Chemical Method,” *Journal of New Materials for Electrochemical Systems*, vol. 14, no. 4, pp. 203–207, 2011.
- [60] Z. F. Tang, R. Wu, P. F. Huang, Q. S. Wang, and C. H. Chen, “Improving the electrochemical performance of Ni-rich cathode material LiNi_{0.815}Co_{0.15}Al_{0.035}O₂ by removing the lithium residues and forming Li₃PO₄ coating layer,” *Journal of Alloys and Compounds*, vol. 693, pp. 1157–1163, 2017.
- [61] W. Liu, H. Guo, M. Qin et al., “Effect of voltage range and BiPO₄ Coating on the electrochemical properties of LiNi_{0.8}Co_{0.15}Al_{0.05}O₂,” *ChemistrySelect*, vol. 3, no. 26, pp. 7660–7666, 2018.
- [62] S. Xia, F. Li, F. Chen, and H. Guo, “Preparation of FePO₄ by liquid-phase method and modification on the surface of LiNi_{0.80}Co_{0.15}Al_{0.05}O₂ cathode material,” *Journal of Alloys and Compounds*, vol. 731, pp. 428–436, 2018.
- [63] W. Xiao, Z. Wang, C. Miao et al., “High performance composite polymer electrolytes doped with spherical-like and honeycomb structural Li_{0.1}Ca_{0.9}TiO₃ particles,” *Frontiers in Chemistry*, vol. 6, pp. 525–531, 2018.
- [64] T. F. Yi, J. Mei, P. P. Peng, and S. Luo, “Facile synthesis of polypyrrole-modified Li₅Cr₇Ti₆O₂₅ with improved rate performance as negative electrode material for Li-ion batteries,” *Composites Part B: Engineering*, vol. 167, pp. 566–572, 2019.
- [65] W. Liu, G. Hu, K. Du, Z. Peng, Y. Cao, and Q. Liu, “Synthesis and characterization of LiCoO₂-coated LiNi_{0.8}Co_{0.15}Al_{0.05}O₂ cathode materials,” *Materials Letters*, vol. 83, pp. 11–13, 2012.
- [66] C. Yang, R. Shao, Y. Mi et al., “Stable interstitial layer to alleviate fatigue fracture of high nickel cathode for lithium-ion batteries,” *Journal of Power Sources*, vol. 376, pp. 200–206, 2018.
- [67] B. Xu, P. Dong, J. Duan, D. Wang, X. Huang, and Y. Zhang, “Regenerating the used LiFePO₄ to high performance cathode via mechanochemical activation assisted V⁵⁺ doping,” *Ceramics International*, vol. 45, no. 9, pp. 11792–11801, 2019.
- [68] J. Chen, L. Zhu, D. Jia et al., “LiNi_{0.8}Co_{0.15}Al_{0.05}O₂ cathodes exhibiting improved capacity retention and thermal stability due to a lithium iron phosphate coating,” *Electrochimica Acta*, vol. 312, pp. 179–187, 2019.
- [69] J. S. Park, A. U. Mane, J. W. Elam, and J. R. Croy, “Amorphous metal fluoride passivation coatings prepared by atomic layer deposition on LiCoO₂ for Li-ion batteries,” *Chemistry of Materials*, vol. 27, no. 6, pp. 1917–1920, 2015.
- [70] P. Yue, Z. Wang, X. Li et al., “The enhanced electrochemical performance of LiNi_{0.6}Co_{0.2}Mn_{0.2}O₂ cathode materials by low temperature fluorine substitution,” *Electrochimica Acta*, vol. 95, pp. 112–118, 2013.
- [71] Z. Zhu, F. Cai, and J. Yu, “Improvement of electrochemical performance for AlF₃-coated Li_{1.3}Mn_{4/6}Ni_{1/6}Co_{1/6}O_{2.40} cathode materials for Li-ion batteries,” *Ionics*, vol. 22, no. 8, pp. 1353–1359, 2016.
- [72] L. Chen, Y. Yang, Z. Wang et al., “Enhanced electrochemical performances and thermal stability of LiNi_{1/3}Co_{1/3}Mn_{1/3}O₂ by surface modification with YF₃,” *Journal of Alloys and Compounds*, vol. 711, pp. 462–472, 2017.
- [73] C. D. Li, Z. L. Yao, J. Xu, P. Tang, and X. Xiong, “Surface-modified Li(Li_{0.2}Mn_{0.54}Ni_{0.13}Co_{0.13})O₂ nanoparticles with LaF₃ as cathode for Li-ion battery,” *Ionics*, vol. 23, no. 3, pp. 549–558, 2017.
- [74] A. Kraysberg, H. Drezner, M. Auinat et al., “Atomic layer deposition of a particularized protective MgF₂ Film on a Li-ion battery LiMn_{1.5}Ni_{0.5}O₄ Cathode powder material,” *ChemNanoMat*, vol. 1, no. 8, pp. 577–585, 2015.
- [75] X. Liu, J. Liu, T. Huang, and A. Yu, “CaF₂-coated Li_{1.2}Mn_{0.54}Ni_{0.13}Co_{0.13}O₂ as cathode materials for Li-ion batteries,” *Electrochimica Acta*, vol. 109, pp. 52–58, 2013.
- [76] S. H. Lee, C. S. Yoon, K. Amine, and Y. K. Sun, “Improvement of long-term cycling performance of Li[Ni_{0.8}Co_{0.15}Al_{0.05}]O₂ by AlF₃ coating,” *Journal of Power Sources*, vol. 234, pp. 201–207, 2013.
- [77] C. Li, M. Wang, B. Xie, H. Ma, and J. Chen, “Enhanced properties of diatomite-based composite phase change materials for thermal energy storage,” *Renewable Energy*, vol. 147, pp. 265–274, 2020.
- [78] W. Liu, X. Tang, M. Qin, G. Li, J. Deng, and X. Huang, “FeF₃-coated LiNi_{0.8}Co_{0.15}Al_{0.05}O₂ cathode materials with improved electrochemical properties,” *Materials Letters*, vol. 185, pp. 96–99, 2016.
- [79] Y. M. Chung and K. S. Ryu, “Surface coating and electrochemical properties of LiNi_{0.8}Co_{0.15}Al_{0.05}O₂ polyaniline composites as an electrode for Li-ion batteries,” *Bulletin of the Korean Chemical Society*, vol. 30, no. 8, pp. 1733–1737, 2009.
- [80] C. H. Lai, D. S. Ashby, T. C. Lin et al., “Application of poly(3-hexylthiophene-2,5-diyl) as a protective coating for high rate cathode materials,” *Chemistry of Materials*, vol. 30, no. 8, pp. 2589–2599, 2018.
- [81] H. Xie, K. Du, G. Hu, Z. Peng, and Y. Cao, “The Role of Sodium in LiNi_{0.8}Co_{0.15}Al_{0.05}O₂ Cathode Material and Its Electrochemical Behaviors,” *The Journal of Physical Chemistry C*, vol. 120, no. 6, pp. 3235–3241, 2016.

- [82] D. Y. Wan, Z. Y. Fan, Y. X. Dong et al., "Effect of metal (Mn, Ti) doping on NCA cathode materials for lithium ion batteries," *Journal of Nanomaterials*, vol. 2018, 9 pages, 2018.
- [83] Q. Q. Qiu, Z. Shadike, Q. C. Wang et al., "Improving the electrochemical performance and structural stability of the $\text{LiNi}_{0.8}\text{Co}_{0.15}\text{Al}_{0.05}\text{O}_2$ cathode material at high-voltage charging through Ti substitution," *ACS Applied Materials & Interfaces*, vol. 11, no. 26, pp. 23213–23221, 2019.
- [84] R. Fang, W. Xiao, C. Miao et al., "Fabrication of Si-SiO₂@-Fe/NC composite from industrial waste AlSiFe powders as high stability anodes for lithium ion batteries," *Electrochimica Acta*, vol. 324, pp. 134860–134869, 2019.
- [85] F. Du, R. Chen, Y. Zhuang et al., "Effect of substitution of cobalt with iron on electrochemical behavior and solid electrolyte interface of $\text{LiNi}_{0.8}\text{Co}_{0.15}\text{Al}_{0.05}\text{O}_2$," *Applied Surface Science*, vol. 484, pp. 374–382, 2019.
- [86] B. Huang, X. Li, Z. Wang, H. Guo, and X. Xiong, "Synthesis of Mg-doped $\text{LiNi}_{0.8}\text{Co}_{0.15}\text{Al}_{0.05}\text{O}_2$ oxide and its electrochemical behavior in high-voltage lithium-ion batteries," *Ceramics International*, vol. 40, no. 8, pp. 13223–13230, 2014.
- [87] W. S. Yoon, K. Y. Chung, J. McBreen, and X. Q. Yang, "A comparative study on structural changes of $\text{LiCo}_{1/3}\text{Ni}_{1/3}\text{Mn}_{1/3}\text{O}_2$ and $\text{LiNi}_{0.8}\text{Co}_{0.15}\text{Al}_{0.05}\text{O}_2$ during first charge using in situ XRD," *Electrochemistry Communications*, vol. 8, no. 8, pp. 1257–1262, 2006.
- [88] Y. Y. Wang, Y. Y. Sun, S. Liu, G. R. Li, and X. P. Gao, "Na-doped $\text{LiNi}_{0.8}\text{Co}_{0.15}\text{Al}_{0.05}\text{O}_2$ with excellent stability of both capacity and potential as cathode materials for Li-ion batteries," *ACS Applied Energy Materials*, vol. 1, no. 8, pp. 3881–3889, 2018.
- [89] H. Liu, M. Wolf, K. Karki et al., "Intergranular cracking as a major cause of long-term capacity fading of layered cathodes," *Nano Letters*, vol. 17, no. 6, pp. 3452–3457, 2017.
- [90] Q. Li, G. Li, C. Fu, D. Luo, J. Fan, and L. Li, "K(+)-doped $\text{Li}_{1.2}\text{Mn}_{0.54}\text{Co}_{0.13}\text{Ni}_{0.13}\text{O}_2$: a novel cathode material with an enhanced cycling stability for lithium-ion batteries," *ACS Applied Materials & Interfaces*, vol. 6, no. 13, pp. 10330–10341, 2014.
- [91] M. N. Ates, Q. Jia, A. Shah, A. Busnaina, S. Mukerjee, and K. M. Abraham, "Mitigation of layered to spinel conversion of a Li-rich layered metal oxide cathode material for Li-ion batteries," *Journal of the Electrochemical Society*, vol. 161, no. 3, pp. A290–A301, 2014.
- [92] J. Zhao, Z. Wang, J. Wang et al., "Anchoring K⁺ in Li⁺ Sites of $\text{LiNi}_{0.8}\text{Co}_{0.15}\text{Al}_{0.05}\text{O}_2$ Cathode material to suppress its structural degradation during high-voltage cycling," *Energy Technology*, vol. 6, no. 12, pp. 2358–2366, 2018.
- [93] L. Zhu, Y. Liu, W. Wu, X. Wu, W. Tang, and Y. Wu, "Surface fluorinated $\text{LiNi}_{0.8}\text{Co}_{0.15}\text{Al}_{0.05}\text{O}_2$ as a positive electrode material for lithium ion batteries," *Journal of Materials Chemistry A*, vol. 3, no. 29, pp. 15156–15162, 2015.
- [94] Y. Huang, S. D. Gong, R. Huang et al., "Polyhedral oligomeric silsesquioxane containing gel polymer electrolyte based on a PMMA matrix," *RSC Advances*, vol. 5, no. 57, pp. 45908–45918, 2015.
- [95] X. Li, F. Kang, W. Shen, and X. Bai, "Improvement of structural stability and electrochemical activity of a cathode material $\text{LiNi}_{0.7}\text{Co}_{0.3}\text{O}_2$ by chlorine doping," *Electrochimica Acta*, vol. 53, no. 4, pp. 1761–1765, 2007.
- [96] W. K. Kim, D. W. Han, W. H. Ryu, S. J. Lim, J. Y. Eom, and H. S. Kwon, "Effects of Cl doping on the structural and electrochemical properties of high voltage $\text{LiMn}_{1.5}\text{Ni}_{0.5}\text{O}_4$ cathode materials for Li-ion batteries," *Journal of Alloys and Compounds*, vol. 592, pp. 48–52, 2014.
- [97] Y. Qi, Y. Huang, D. Jia, S. J. Bao, and Z. P. Guo, "Preparation and characterization of novel spinel $\text{Li}_4\text{Ti}_5\text{O}_{12-x}\text{Br}_x$ anode materials," *Electrochimica Acta*, vol. 54, no. 21, pp. 4772–4776, 2009.
- [98] T. F. Yi, Y. R. Zhu, W. Tao, S. Luo, Y. Xie, and X. F. Li, "Recent advances in the research of $\text{MLi}_2\text{Ti}_6\text{O}_{14}$ (M = 2Na, Sr, Ba, Pb) anode materials for Li-ion batteries," *Journal of Power Sources*, vol. 399, pp. 26–41, 2018.
- [99] Y. Yan, Y. X. Yin, S. Xin, Y. G. Guo, and L. J. Wan, "Ionothermal synthesis of sulfur-doped porous carbons hybridized with graphene as superior anode materials for lithium-ion batteries," *Chemical Communications*, vol. 48, no. 86, pp. 10663–10665, 2012.
- [100] H. Z. Zhang, Q. Q. Qiao, G. R. Li, and X. P. Gao, "PO₄³⁻ polyanion-doping for stabilizing Li-rich layered oxides as cathode materials for advanced lithium-ion batteries," *Journal of Materials Chemistry A*, vol. 2, no. 20, pp. 7454–7460, 2014.
- [101] S. He, A. Wei, W. Li et al., "An in-depth analysis detailing the structural and electrochemical properties within Br⁻ modified $\text{LiNi}_{0.815}\text{Co}_{0.15}\text{Al}_{0.035}\text{O}_2$ (NCA) cathode material," *Electrochimica Acta*, vol. 318, pp. 362–373, 2019.
- [102] T. Chen, X. Li, H. Wang et al., "The effect of gradient boracic polyanion-doping on structure, morphology, and cycling performance of Ni-rich $\text{LiNi}_{0.8}\text{Co}_{0.15}\text{Al}_{0.05}\text{O}_2$ cathode material," *Journal of Power Sources*, vol. 374, pp. 1–11, 2018.

